

Fast Monomers: Factors Affecting the Inherent Reactivity of Acrylate Monomers in Photoinitiated Acrylate Polymerization

Johan F. G. A. Jansen,* Aylvin A. Dias, Marko Dorsch, and Betty Coussens

DSM Research, P.O. Box 18, 6160 MD Geleen, The Netherlands

Received December 26, 2002; Revised Manuscript Received April 3, 2003

ABSTRACT: A systematic study on the effect of molecular structure on the photoinitiated polymerization of acrylates was undertaken. Initially, the research was focused on the effect of hydrogen bonding, and it was found that preorganization via hydrogen bonding enhances the maximum rate of polymerization (R_p). This hydrogen bonding facilitated preorganization also affected the tacticity of the resultant polymer. Next, the effect of polarity as represented by the calculated dipole moment (μ_{calc}) of a given monomer was investigated. A direct linear correlation between R_p and the calculated Boltzmann-averaged dipole moment (μ_{calc}) was observed. The R_p – μ_{calc} correlation holds for pure monomers, mixtures of monomers, and even mixtures of monomers with inert solvents. This correlation enables the rational design of monomers with a required reactivity. In addition, these studies suggest that the propagation step of polymerization is influenced by hydrogen bonding while the dipole moment influences the termination rate constant. These two mechanistic explanations can be regarded as complementary factors that influence the speed of acrylate polymerization.

Introduction

Photoinitiated polymerization of acrylates and methacrylates is one of the most efficient processes for the rapid production of polymeric cross-linked materials with defined properties. This very efficiency is the reason that photoinitiated polymerization is widely employed in the performance applications where emphasis is put on the mechanical as well as optical properties. These applications are typically dental restorative fillers, fiber-optic coatings, optical adhesives, aspherical lenses for CD applications, and the preparation of contact lenses.¹

Although the use of photoinitiated polymerization is widespread, fundamental understanding of factors that affect polymerization speed remains limited. The preferred method to increase the polymerization rate is to increase photoinitiator concentration, use of more efficient photoinitiators, or to increase reactive group functionality of the oligomers and monomers used. Regarding mechanistic kinetic investigations, few detailed investigations can be found for acrylates. However, with methacrylates kinetic investigations² have been performed, using calorimetric methods (photodifferential scanning calorimetry (photo-DSC) or spectroscopically, e.g., real-time Fourier transform infrared spectroscopy (RT-FTIR)). Investigations using these time-resolved techniques have led to several models like bimolecular termination combined with reaction diffusion-controlled kinetics,³ monomolecular termination in the glassy region,⁴ primary radical termination,⁵ chain length-dependent termination,⁶ random walk for heterogeneity,⁷ primary cyclization,⁸ and the effect of monomer functionality.⁹ It is assumed that acrylates will react according to similar pathways as for methacrylates studied thus far. However, there is enough evidence in the literature that acrylates behave differently. Berchthold et al. found a notable difference in the addition of small amounts of thiols as chain transfer

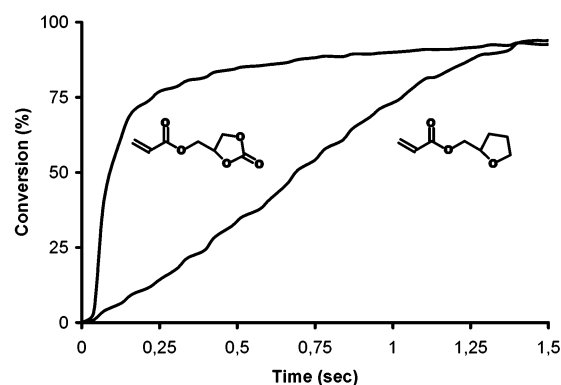


Figure 1. RT-FTIR time conversion profiles of tetrahydrofurfuryl acrylate **36** and glycerolcarbonate acrylate **57** under nitrogen initiated with 1% w/w hydroxy cyclohexyl phenyl ketone.

agents, which have a large impact on the polymerization rate of methacrylates but almost no influence on the polymerization rate of the corresponding acrylates.¹⁰

Comprehension of the influence of molecular structure on acrylate reactivity has been sought ever since the first publications with acrylates and methacrylates that reported high inherent reactivities. Figure 1 illustrates the differences in polymerization behavior observed with RT-FTIR of acrylates with different molecular structures.

Deckers¹¹ report on acrylates with a very high intrinsic reactivity assigned importance to hydrogen abstraction as a potential reason for high R_p . Andrzejewska¹² reported a heteroatom effect in the side chain which led to higher reactivity. Enhanced polymerization rates were also found by performing the photoinitiated polymerization in ordered liquid crystalline phases as was elegantly demonstrated by Guymon.¹³ These results stimulated our effort to understand, on a molecular level, the features that contribute to the high intrinsic polymerization reactivity of acrylates. On the basis of such a fundamental understanding, the rational design of acrylates and blends thereof with required designed

* To whom correspondence should be addressed. E-mail: johan-fga.jansen@dsm.com.

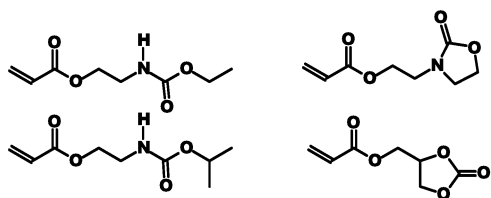


Figure 2. Acrylate monomers with a high R_p as reported by Decker.

reactivities can be envisaged, instead of the trial-and-error approach applied so far. The pioneering work of Decker, demonstrating that the molecules depicted in Figure 2 polymerized with a high R_p ,¹¹ served as starting point for our investigations.

On the basis of these results, we decided to focus our research on the influence of hydrogen bonding and polarity (as defined by the calculated dipole moment) as starting rationales for the high polymerization rates observed in the literature.¹⁴ New high reactivity acrylate monomers are introduced as part of the study.

Experimental Section

Most of the monomer preparations are straightforward organic procedures; hence, only one representative example is given. Where the synthesis of a monomer is more complicated, the full experimental details are given. All the chemicals were used as obtained from Aldrich or other sources, except THF, which was distilled over Na/benzophenone, dichloromethane, which was distilled over P_2O_5 , and pyridine, triethylamine, and acryloyl chloride, which were freshly distilled prior to use.

The RT-FTIR setup employed is a transmission reflection cell with heating and nitrogen inerting capability.¹⁵ A 200 W medium-pressure mercury lamp that delivered a UV light intensity of 135 mW/cm² at the sample position as measured with a Solatrel Solo-scope 1 was employed. The sample thickness for nonlaminated samples was 7 μ m, unless otherwise stated. A nitrogen purge was applied for at least 5 min prior to RT-FTIR measurements, and the temperature was maintained at 25.0 ± 1.0 °C. All RT-FTIR measurements were performed in triplicate, with a spectral sampling rate of 0.038 s per IR spectrum (at 4 cm⁻¹ spectral resolution). In the rare cases where RT-FTIR experiments were performed on samples that were laminated, the light intensity at the sample was 45 mW/cm² and the sample thickness was 50 μ m. Differentiation in order to obtain R_p was performed with an in-house-developed Fortran program using the following constraints: maximum error in time resolution 0.005 s, maximum error in conversion 2%, and the fit should be differentiable twice. For the kinetic measurements a summation, per nanometer, of the emission spectrum of the lamp combined with the absorption spectrum of the photoinitiator was taken for the calculation of the amount of the photons absorbed. In the kinetic analysis an optically thin film was assumed, thereby eliminating the need to know the exact film thickness, i.e., $R_p = (k_p/k_t^{1/2})[M] - (\varphi I_0 \epsilon [PI])^{1/2}$ can be used instead of $R_p = (k_p/k_t^{1/2})[M](\varphi I_0(1 - 10^{-d\epsilon[PI]}))^{1/2}$. The rest of the kinetic analysis was performed assuming steady-state conditions as described by Decker.¹⁶

All RT-FTIR measurements were performed employing 1 wt % Irgacure 184 (2-hydroxycyclohexyl phenyl ketone, HCPK, Ciba) as the photoinitiator. All photoinitiated polymerizations were performed to an acrylate double bond conversion >96% (based on IR). The conversion was cross-checked with selected samples by ¹H NMR, ¹³C NMR, and Raman spectroscopy at various conversions. The values obtained were in good agreement (within 3% error, although the NMR techniques tend to become less accurate at high conversions, i.e., above 90% double bond conversion). Photoinitiated polymerizations of the methacrylate monomers in order to determine tacticity of the resultant polymers were performed under nitrogen using a

Fusion UV curing conveyor system equipped with F600 D 6 kW bulbs. The samples were given the dose required to reach >97% conversion (determined by NMR). Employing higher doses resulted in the appearance of unwanted and yet unidentified signals, which may be attributed to photoinitiator and polymer/oligomer based secondary hydrogen abstraction reactions. In fact, even with lauryl methacrylate, insoluble gel particles were obtained upon using a high UV dose.¹⁷ The tacticity was determined by ¹³C NMR using a Bruker ARX 400 in DMSO-*d*₆ at 80 °C. A Bruker AMX 200 was used for the standard ¹H and ¹³C NMR measurements employing DMSO-*d*₆ as solvent.

Calculation of Dipole Moments. Boltzmann-averaged dipole moments (μ_{calc}) were calculated in the following way. First, for a given acrylate a set of starting configurations that considered all possible bond rotations were generated. This was done by means of the Discover 95 program.^{18a} Torsional angles were considered to depend on the type of bond; e.g., for a bond between two sp³ carbons the angles taken into account are those corresponding to the two possible gauche conformations and the trans conformation. The number of configurations generated is thus dependent on both the number of bonds and their type. For example, for five sp³-like bonds one has 3⁵ = 243 configurations. As a consequence, for some of the acrylates, the total number of configurations was a few thousand. All these configurations were then minimized at the AM1 level using MOPAC 6.0 with the convergence criterion for the maximum gradient (GNORM) set to 0.05. The resulting structures were sorted by energy, and only the unique structures having a heat of formation differing less than 3 kcal/mol from the heat of formation of the global minimum structure were retained. Whether or not structures were unique was determined by comparing their heats of formation and their dipole moments in the following way. First, structures were considered to be identical if their heats of formation differ at most 0.01 kcal/mol. Nevertheless, structures that were considered to be identical on the basis of this energy criterion were considered to be unique if their dipole moments differed more than 0.2 D. Having determined the unique structures, the Boltzmann-weighted dipole moment was consequently evaluated according to the formula

$$\langle \mu_{\text{calc}} \rangle = \frac{\sum_j D_j \frac{e^{-\Delta H_j/RT}}{\sum_i e^{-\Delta H_i/RT}}}{\sum_j p_j} = \sum_j D_j p_j$$

with D_j the dipole moment of conformation j , ΔH_j the difference between the heat of formation of conformation j and the heat of formation of the global minimum conformation, T the absolute temperature, and R the Boltzmann constant; p_j is the probability of finding the molecule in conformation j at the temperature T . T is set to 298.15 K. The summation over j runs over all unique structures. Sorting of structures, retaining only the unique ones and the calculation of $\langle \mu_{\text{calc}} \rangle$ was done by means of a FORTRAN program developed in-house.

The advantage in considering the Boltzmann-weighted dipole moment instead of the dipole moment of the global minimum structure is that the former approach takes into account the fact that several conformations can be accessible at T . It is implicit that when the dipole moments of the accessible conformations are significantly different, the value of $\langle \mu_{\text{calc}} \rangle$ may differ significantly from the dipole moment of the global minimum. The Boltzmann-weighted dipole moment (μ_{calc}) therefore provides a much more realistic description of the system.

Calculation of Radical Charges. ESP charge calculations have been performed with the Gaussian98 package^{18b} at the B3LYP/6-31G* level. In the gas phase a full geometry optimization was carried out whereas the ESP charges obtained for $D = 0.9$ and $D = 5$ were obtained by performing single-point calculations on the B3LYP/6-31G* gas-phase geometry using the SCI-PCM method employing the default isodensity value of 0.0004 au.

Synthesis of Ethyl-*O*-urethane-*N*-ethyl Acrylate¹⁹ 5: Typical Procedure. To a stirred cooled solution at 0 °C of 14.22 g (107 mmol) of *N*-2-hydroxyethyl-*O*-ethylurethane and 8.45 g (107 mmol) of pyridine in 300 mL of THF, purged with dry air, was slowly added 10.1 g (112 mmol, 1.05 equiv) of acryloyl chloride while maintaining the temperature below 5 °C. After the addition was complete, the reaction mixture was allowed to warm to room temperature and was then stirred at this temperature for an additional 6 h.

Workup. The pyridinium salt was filtered off, followed by a quick wash with 20 mL of water, 0.1 N hydrochloric acid, saturated NaHCO₃ solution, and brine (where the separation was tedious diethyl ether was added). After drying over Na₂SO₄, THF was removed in vacuo, yielding 6.1 g (33 mmol, 31%) of ethyl-*O*-urethane-*N*-ethyl acrylate as crude product with a purity based on NMR of 97%.

Alternative Workup. The pyridinium salt was filtered off, followed by removal of the THF at a vacuum of 10 mbar, yielding 18.2 g (97 mmol, 90%) of crude ethyl-*O*-urethane-*N*-ethyl acrylate with a purity based on NMR of 85%.

Distillation Procedure. 1 g of the crude product was used to determine the boiling point of the acrylate by slowly raising the temperature at a vacuum of 2 mbar until all remaining THF, pyridine, and acryloyl chloride were distilled. At 135 °C the boiling temperature remained constant for approximately 10 min before the acrylate started to polymerize in the distillation flask due to the prolonged heating. Next, 15 g of the remaining crude product was distilled by quickly raising the temperature to 150 °C, taking a large first run, followed by the product. As soon as any polymerization was noticed or suspected (fumes), the distillation was stopped, yielding 9 g of product, which still contained some trace impurities presumably due to the stabilizer used in the acryloyl chloride. To obtain pure product, i.e., no other signals detected on GC, the distillation had to be repeated three times after which only 2 g (10% yield) of pure ethyl-*O*-urethane-*N*-ethyl acrylate was obtained. ¹H NMR (CDCl₃, 200 MHz): δ (ppm) 6.44 (dd; 1H; *J* = 17.22; *J* = 1.48), 6.15 (dd; 1H; *J* = 10.33; *J* = 17.22), 5.88 (dd; 1H; *J* = 10.33; *J* = 1.48), 5.72 (s br; 1H; NH), 4.23 (m; 4H), 3.21 (dt; 2H; *J* = 6.77), 1.14 (t; 3H; *J* = 6.85). ¹³C NMR (CDCl₃, 50 MHz): δ (ppm) 166.7 (s), 157.0 (s), 132.0 (t), 128.8 (d), 63.6 (t), 63.0 (t), 36.5 (t), 15.8 (q). IR (neat): abs cm⁻¹, 3345 (N-H), 1728 (C=O), 1534 (N-H def), 810 (C=C-H).

All liquid compounds were distilled at least three times before they were obtained in a pure form, except the ureas, which were recrystallized three times. Where bulb-to-bulb distillation was used approximately five distillations are required; however, the overall yields are higher due to the lower temperatures employed (for ethyl-*O*-urethane-*N*-ethyl acrylate; 23% overall yield). Another possible distillation procedure from which stabilizer-free acrylate can be obtained is distilling carefully over powdered KOH. However, this procedure is only applicable where the acrylate side group is stable to base. In our hands, neither inhibitor removing columns nor chromatography yielded inhibitor-free acrylates.

Synthesis of 6-Ring Cyclic Carbonate Acrylate 58. **Synthesis of Trimethylolpropane Carbonate (6-CCOH).** A 3 L round-bottom three-neck flask, equipped with a mechanical stirrer, distillation setup, and a small dropping funnel, was charged with 1000 g of trimethylolpropane and 920 g of diethyl carbonate. After heating the reaction mixture to 110 °C, 0.841 g of KOH dissolved in 2 mL of water was added dropwise, after which the temperature was raised to 120 °C. The reaction mixture was stirred at 120 °C for 12 h, during which approximately 400 g of ethanol was distilled over. After distilling off the remaining ethanol at a reduced pressure (800 mbar), the composition of the reaction mixture was checked by GC. This revealed that still 8% trimethylolpropane remained in the reaction mixture. Therefore, 100 g of diethyl carbonate and 0.4 g of KOH dissolved in water was added, and the reaction was continued at 120 °C for an additional 8 h, after which the ethanol and excess diethyl carbonate were stripped off and the conversion checked by GC. This procedure had to be repeated two times before full conversion (based on GC) of trimethylolpropane was reached. The remaining polymeric trimethylol-

propane carbonate was carefully neutralized with *p*-toluenesulfonic acid over a neutralization period off at least 1 h. This neutralization step is very critical. In basic conditions the depolymerization of the oligomeric polycarbonate hardly occurs. However, in an acidic environment a rapid, acid-catalyzed decarboxylation occurs as well, after which a hydroxy functional oxetane can be isolated.

The polymeric trimethylolpropane carbonate was transferred into a preheated (150 °C) dropping funnel. The polymer was dropped slowly (maximum rate 100 mL/h) into a heated (250 °C) 250 mL round-bottom flask equipped with a distillation setup and charged with 1 g of tin flakes under a reduced pressure (8 mbar). Depolymerization occurred immediately, and the crude product was distilled over. As soon as the depolymerization was no longer spontaneous, the reaction was stopped and only 50% crude product was obtained. Unfortunately, the crude product obtained in this way still contained some (15%) hydroxy functional oxetane. All our attempts to separate these two alcohols by distillation failed. Often the amount of oxetane increased during distillation, which might indicate a temperature-induced decarboxylation reaction. Therefore, we decided to continue with the crude alcohol and purify the acrylate. It should be noted that the NMR spectra of the oxetane and the cyclic carbonate are similar; at first glance, the weak carbonyl absorption in ¹³C NMR at 154.8 ppm and the ethyl CH₂ are the distinct differences. Carbonate (6-CCOH) ¹H NMR (DMSO-*d*₆): 5.00 (t, *J* = 5.2 Hz, 1H), 4.20 (AB, *ν* = 15.2 Hz, *J* = 10.2 Hz, 4H), 3.38 (d, *J* = 5.2, 2H), 1.37 (q, *J* = 7.6 Hz, 2H), 0.82 (t, *J* = 7.6 Hz, 3H). ¹³C NMR (DMSO-*d*₆): 154.5 (s), 76.6 (t), 61.8 (t), 35.0 (s), 21.8 (t), 7.2 (q). IR (neat) cm⁻¹: 1734. For comparison, the ¹H NMR spectrum of the oxetane: ¹H NMR (DMSO-*d*₆): 5.00 (t, *J* = 5.3 Hz, 1H), 4.22 (AB, *ν* = 21.4 Hz, *J* = 5.6 Hz, 4H), 3.48 (d, *J* = 5.3, 2H), 1.62 (q, *J* = 7.6 Hz, 2H), 0.83 (t, *J* = 7.6 Hz, 3H).

6-Ring Carbonate Acrylate 58. 100 g (0.63 mol) of 6CCOH was dissolved in 1 L of dry CH₂Cl₂ at room temperature, and 70 g (0.7 mol) of triethylamine was added, after which the reaction mixture was cooled to 0 °C. 60 g (0.66 mol) of acryloyl chloride was dissolved in 1 L of CH₂Cl₂, and this solution was added dropwise to the reaction mixture while the temperature was maintained between 0 and 5 °C. After the addition was complete the reaction mixture was stirred for an additional 2 h between 0 and 5 °C before the reaction mixture was allowed to warm to room temperature overnight. Filtration followed by evaporation of the solvents yielded 140 g of crude product. The distillation procedure described above was followed and after four distillations (195 °C, 0.1 mbar! so a severe risk of acrylate polymerization during the distillation exits); 10 g (46 mmol, 8%) of pure 6-ring carbonate acrylate **58** acrylate was obtained. ¹H NMR (CDCl₃, 200 MHz): δ (ppm) 6.44 (dd; 1H; *J* = 17.22; *J* = 1.48), 6.15 (dd; 1H; *J* = 10.33; *J* = 17.22), 5.88 (dd; 1H; *J* = 10.33; *J* = 1.48), 4.3–4.1 (m, 6H) 1.40, q, *J* = 7.6 Hz, 2H) 0.85 (t, *J* = 7.6 Hz, 3H). ¹³C NMR (CDCl₃, 50 MHz): δ (ppm) 166.5 (s), 148.3 (s), 132.0 (t), 128.8 (d), 72.5 (t), 62.9 (t), 34.6 (s), 23.3 (t), 7.3 (q). IR (neat): abs cm⁻¹, 1730 (C=O broad) 810 (C=C-H). After all the difficulties with the synthesis of this alcohol we contacted Bayer.²⁰ They confirmed that the synthesis is not a trivial matter and kindly sent us a sample of this 6-ring carbonate alcohol.

Synthesis of Carbonate Urethane Acrylate 65. **Synthesis²¹ of Glycerol Carbonate 62:** Procedure 1. A round-bottom flask charged with 725 g (7.7 mol) of glycerol **60**, 500 g of ethylene carbonate, and 0.4 g of NaOH was stirred at 140 °C for 2 h. Neutralization with *p*-toluenesulfonic acid to pH = 6 was followed by distilling off the ethylene glycol. Next, 250 g of ethylene carbonate and 0.4 g of NaOH were added, and the reaction mixture was stirred again at 140 °C for 2 h. This procedure was repeated twice, after which the neutralization was performed to pH = 5. At this acidity the distillation of the product can be performed at 160 °C at 0.01 mbar, yielding 650 g (5.5 mol, 70%) of glycerol carbonate with a purity >97% (pure by NMR). On the basis of GC, the impurities that remained were mainly glycerol, glycidol, and some oligomeric material, which can be removed by two distillations.

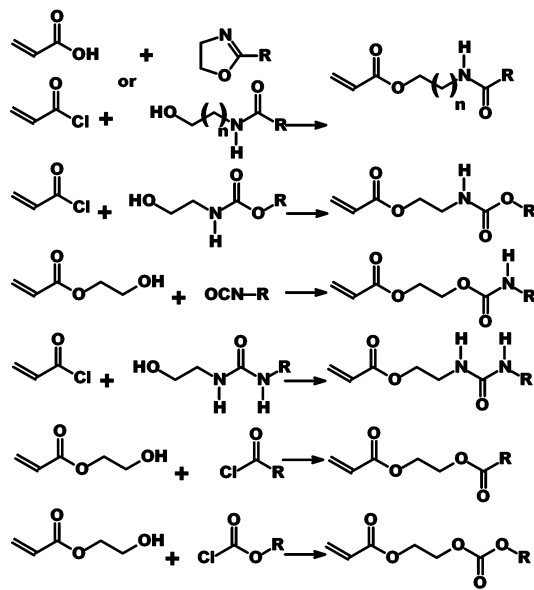
Procedure 2. A round-bottom flask was charged with 45 g (0.34 mol) of 3-allyl-1,2-propanediol **61**, 250 mL of CH_2Cl_2 , and 130 mL of triethylamine (0.9 mol), and the reaction mixture was cooled to 0 °C. 200 mL of a solution of phosgene in toluene (20% in toluene, 0.4 mol) was added dropwise at such a rate that the reaction temperature was kept below 10 °C. After the addition the mixture was stirred for a further 2 h at 0 °C before it was allowed to warm to room temperature overnight. Washing with water, 5% sodium bicarbonate solution, and water, drying over Na_2SO_4 , and evaporation of the solvent followed by bulb-to-bulb distillations yielded 36 g (0.22 mol, 67%) of the allyl protected cyclic carbonate. 24.5 g (0.16 mol) of the allyl protected cyclic carbonate was dissolved in 300 mL of methanol. After stopping the stirrer, nitrogen was flushed for 10 min followed by the addition of 3.7 g of Pd/C (10% Pd) and subsequently 2.5 g of *p*-toluenesulfonic acid. The reaction mixture was then stirred at room temperature, and the conversion was monitored by ^1H NMR. After 6 days the deprotection was complete. The reaction mixture was filtered over neutral Al_2O_3 . The Al_2O_3 was subsequently rinsed with 500 mL of methanol. The methanol fractions were combined and concentrated. Distillation (0.01 mbar, 160–170 °C) yielded 14 g (0.13 mol, 80%) of pure glycerol carbonate **62** (purity >99%, GC). ^1H NMR (CDCl_3 , 200 MHz): δ (ppm) 5.4 (s br; 1H), 4.9–4.8 (m; 1H), 4.6–4.4 (m; 2H), 3.9–3.5 (m, 2H). ^{13}C NMR (CDCl_3 , 50 MHz): δ (ppm) 155.5 (s), 77.1 (d), 66.0 (t) 60.6 (t). IR (neat): abs cm^{-1} , 1734 (C=O broad).

Synthesis of the Glycerol Carbonate Active Ester 63. A round-bottom flask was charged with 38.23 g (0.322 mol) of glycerol carbonate **62** and 28 g (0.35 mol) of pyridine and cooled to 0 °C before 50.35 g (0.322 mol) of phenyl chloroformate was added dropwise at such a rate that the reaction temperature was kept below 5 °C. After the addition was complete the reaction mixture was kept at this temperature overnight. The salts formed were filtered off, and the remaining CH_2Cl_2 layer was washed with water, dilute hydrochloric acid (0.01 N), water, a sodium bicarbonate solution, water, and brine followed by drying over Na_2SO_4 , and evaporation of the solvent yielded 66.8 g of the active ester **63** (0.28 mol, 87%), which was pure enough to be employed in the subsequent reaction. ^1H NMR (DMSO, 200 MHz): δ (ppm) 7.7–7.4 (m; 5H), 5.2–5.1 (m; 1H), 4.7–4.3 (m; 4H).

Synthesis of Hydroxyurethane Glycerol Carbonate 64. 17.55 g (74 mmol) of active ester **63** was dissolved in 200 mL of THF and cooled to –5 °C, and 4.5 g (74 mmol) of ethanolamine in 200 mL of dry THF was added dropwise, while maintaining the temperature below 0 °C. (If performed slowly, no exotherm should be noticeable.) After the addition is complete (approximately 3 h) the reaction mixture was stirred for 3 days at 0 °C before the temperature was slowly raised to room temperature. The THF layer is diluted with ether and extracted with 3 \times 100 mL of distilled water. The combined water layers were washed with CH_2Cl_2 , after which the water is evaporated in vacuo, yielding 13.6 g (67 mmol, 90%) of hydroxyurethane glycerol carbonate **64**. ^1H NMR (DMSO- d_6 , 200 MHz): δ (ppm) 7.5 (s br; 1H), 5.3 (s br; 1H), 4.9–4.8 (m; 1H), 4.7–4.4 (m; 4H), 3.9–3.5 (m, 4H). ^{13}C NMR (DMSO- d_6 , 50 MHz): δ (ppm) 161.7 (s), 155.9 (s), 75.8 (d), 65.7 (t) 63.8 (t), 62.7 (t), 45.5 (t). IR (neat): abs cm^{-1} , 3400–3100 (NH, OH), 1730 (C=O broad). It is difficult to remove the last traces of water; therefore, a larger excess acryloyl chloride is used in the next step.

Synthesis of Glycerol Carbonate Urethane Acrylate 65. To a stirred cooled solution at 0 °C, purged with dry air, of 5.2 g (25 mmol) of hydroxyurethane glycerol carbonate **64** and 8 g (100 mmol) of pyridine in 300 mL of THF was slowly added 7 g (76 mmol, 3 equiv) of acryloyl chloride in 100 mL of THF while maintaining the temperature below 5 °C. After the addition was complete, the reaction mixture was allowed to warm slowly to room temperature and was stirred at room temperature for an additional 6 h. After the pyridinium salt was filtered off, the mixture was cooled to 0 °C before the mixture was filtered again. The excesses employed were evaporated off (100 °C, 0.7 mbar), followed by several distillations yielding 0.9 g of glycerol carbonate urethane acrylate

Scheme 1. Synthesis of Monomers Capable of Hydrogen Bonding and Their Non-Hydrogen-Bonding Control Monomers



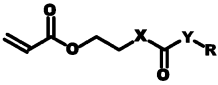
65 (3.5 mmol, 15%). ^1H NMR (DMSO, 200 MHz): δ (ppm) 7.5 (t; 1H; $J = 5.7$ Hz), 6.44 (dd; 1H; $J = 17.22$; $J = 1.48$), 6.15 (dd; 1H; $J = 10.33$; $J = 17.22$), 5.88 (dd; 1H; $J = 10.33$; $J = 1.48$), 5.0 (m; 1H), 4.6–4.0 (m; 6H), 3.3–3.1 (m, 2H). ^{13}C NMR (DMSO, 50 MHz): δ (ppm) 167.0 (s), 161.7 (s), 155.9 (s), 131.7 (t), 128.4 (d), 74.8 (d), 65.9 (t), 63.4 (t), 62.9 (t), 45.4 (t). IR (neat): abs cm^{-1} , 3200 (NH), 1730 (C=O broad), 810 (C=C–H).

Results and Discussion

Monomers Capable of Hydrogen Bonding. The high reactivity of the urethane ethyl acrylates depicted in Figure 2 suggested that the high R_p of these monomers could be attributed to hydrogen bonding. To evaluate this hypothesis, we performed initial curing experiments with undecyl amide *N*-ethyl acrylate, a monomer capable of hydrogen bonding, and pentyl amide *N*-methyl *N*-ethyl acrylate as a non-hydrogen-bonding, control monomer with the same secondary functionality. The R_p of these acrylate monomers were determined by RT-FTIR. The R_p of the hydrogen-bonding monomer, undecyl amide *N*-ethyl acrylate, was 9 mol/(L s) while the non-hydrogen-bonding analogue pentyl amide *N*-methyl *N*-ethyl acrylate gave a much lower R_p of 1.9 mol/(L s). These results are indicative of the possible importance of hydrogen bonding on the rate of acrylate photoinitiated polymerization. These encouraging initial results triggered us to systematically vary the nature of the secondary group of the acrylate. As monomers capable of hydrogen-bonding amide, urethane, “inverted urethane”, and urea acrylates were prepared. Analogous ester and carbonate acrylates were synthesized and evaluated as control compounds since as they possess no capability for hydrogen bonding. The synthesis of these compounds is shown in Scheme 1.

The preparation of amide ethyl acrylates via the oxazoline precursor was rendered difficult by purification of the end product. This purification is difficult because approximately 1% of the corresponding alkyl ester ethyl acrylamide is formed during synthesis, and selective distillation of the amide ethyl acrylate was very difficult. Since we were unable to remove this byproduct by chromatography or distillation, we abandoned this

Table 1. R_p (mol/(L s)) of Photoinitiated Polymerization of Monomers Capable of Hydrogen Bonding and the Non-Hydrogen-Bonding Control Compounds Determined by RT-FTIR with a Light Intensity of 135 mW/cm² (Medium-Pressure Mercury Lamp)

				R (Compound no)			
X	Y	C ₂ H ₅	C ₄ H ₉	C ₆ H ₁₃	C ₈ H ₁₇		
N	-	23.5 (1)	19.1 (2)	13.6 (3)	9.3 (4)		
N	O	16.1 (5)	9.7 (6)	5 (7)	4.5 (8)		
O	N	15.9 (9)	15.2 (10)	14.5 (11)	14.0 (12)		
N	N	25.2 22.2* (13)	- 18.2* (14)	- 18.0* (15)	- 17.9* (16)		
O	-	4.4 (17)	3.8 (18)	3.5 (19)	3.2 (20)		
O	O	6.5 (21)	5.7 (22)	5.5 (23)	5.4 (24)		

*Measured at 50°C due to their melting points

otherwise versatile synthetic route. To obtain the compounds with high purity (>99% based on GC), all the syntheses were performed via the acid chloride, chloroformate, or isocyanate starting materials. All the syntheses gave the crude compounds in yields between 70 and 90%. Most of the alkyl urea ethyl acrylates (except ethyl urea ethyl acrylate) were solids at room temperature. As a consequence, the R_p of the ureas were determined at 50 °C when all the samples were in their liquid state. In Table 1 the R_p of amide, urethane, "inverted urethane", and urea acrylates as well as their non-hydrogen-bonding analogues are shown.

It is evident from Table 1 that monomers capable of forming hydrogen bonds generally exhibit higher R_p 's compared to their non-hydrogen-bonding analogues. Comparing the ethyl-substituted compounds around 3–6 times higher R_p 's are observed. These findings demonstrate that hydrogen bonding has a pronounced effect on the maximum rate of these photoinitiated acrylate polymerizations.

How can these effects be rationalized? One explanation is that via hydrogen bonding the monomers are dynamically noncovalently connected, i.e., behave partly like a difunctional species. Such a scenario is known for methacrylic acid,²² and in that case it has been established that the propagation rate constant (k_p) was hardly influenced but that the termination rate constant (k_t) has been dramatically reduced.

Another plausible explanation for these enhanced R_p 's is that hydrogen bonding facilitates preorganization in these acrylates, thereby forcing the acrylate double bonds in close proximity to each other. As a consequence, the propagation reaction rate constant (k_p) will be enhanced resulting in higher R_p . Organization of monomers via hydrogen bonding by either explanation has several consequences.

There should be a critical distance between the acrylate group and the hydrogen-bonding moiety (alkyl bridge length) beyond which there is no effect on R_p in the case of the preorganization theory, whereas in the

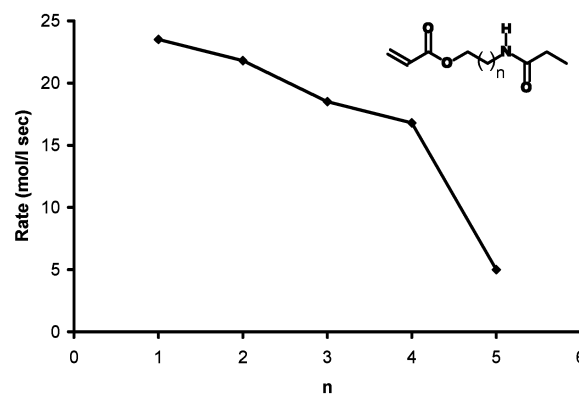


Figure 3. Effect of varying the bridge length between acrylate and amide group on the maximum rate of photoinitiated acrylate polymerization.

case of a noncovalent connection no effect on R_p is expected as the amount of "bifunctional" material is independent of the bridge but only depended on the association strength.

Contrary to normal polymerizations, which exhibit Arrhenius type behavior, increasing the temperature should lead to a deviation from this behavior since at elevated temperatures the extent of hydrogen bonding is reduced. So according to both explanations, lower R_p 's should be found at elevated temperatures.

Preorganization might influence the tacticity of the polymer. Therefore, the tacticity of the resultant polymer could be different when compared with polyacrylates prepared from monomers, incapable of hydrogen bonding. However, in the case of a noncovalent connection again no effect is expected, in this case the acrylate monomers would not be aligned and the normal tacticity should be found.

Changes in tacticity would also discriminate between inter- and intramolecular hydrogen bonding, thereby adding further validity to the preorganization concept. Only with preorganization via intermolecular hydrogen bonding can increased isotacticity be expected. In the case of intramolecular hydrogen bonding it is still possible that R_p enhancements could be found due to a charging of the acrylate double bond; however, no effect on the tacticity would be expected. As another alternative explanation for the enhanced R_p 's, the higher viscosity of the hydrogen-bonding monomers could be proposed. However, changes in tacticity cannot be explained by this theory.

Effect of Bridge Length. As mentioned earlier, one consequence of preorganization is that when the hydrogen-bonding moiety is at a larger distance from the reactive acrylate group, there will be a critical distance beyond which the preorganization due to the hydrogen bonding will have little or no effect on R_p . This is because conformational mobility of the skeletal bonds between the hydrogen-bonding moiety, and the acrylate double bond will reach a level whereby the acrylate double bond can be regarded as isolated from the hydrogen-bonding moiety. Verification of this prediction based on the preorganization theory was done by preparing and evaluating several ethyl amide *N*-alkyl acrylates, in which the alkyl chain was varied in length from ethyl to hexyl (compounds **1**, **25**, **26**, **27**, **28**). The results of these RT-FTIR experiments are shown in Figure 3.

The R_p 's of the ethyl amide *N*-alkyl acrylates are gradually reduced going from ethyl to pentyl, in line

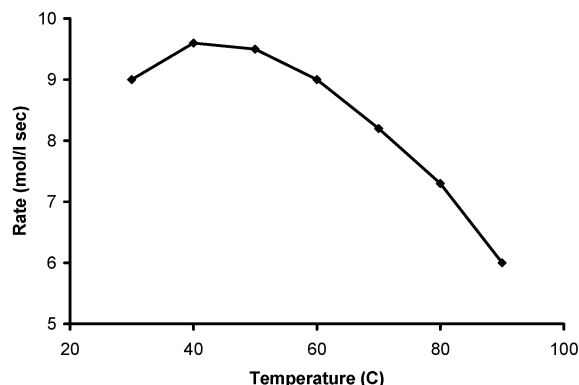


Figure 4. Dependency of the R_p of undecyl amide *N*-ethyl acrylate on the reaction temperature.

with the theory that the effect of the hydrogen bonding will be reduced at a larger distance from the acrylate group. Furthermore, ethyl amide *N*-hexyl acrylate exhibits a R_p similar to monomers not capable of forming hydrogen bonds like the ester and carbonate functional acrylates in Table 1. The occurrence of such a critical distance encourages our belief in the preorganization of acrylate monomers via hydrogen bonding instead of the noncovalent connection theory.

Effect of Temperature. It is recognized that when reactions are performed at higher temperatures, higher rates will be observed this is the so-called Arrhenius behavior. However, if the high R_p is due to preorganization via hydrogen bonding or via a noncovalent connection, at higher temperatures where the extent of hydrogen bonding is reduced, one can expect lower R_p . This reasoning was put to the test with RT-FTIR experiments performed at elevated temperatures. To avoid problems associated with thin films and monomer evaporation at elevated temperatures, we used the high boiling undecyl amide *N*-ethyl acrylate as a monomer capable of hydrogen bonding, and as a control we employed lauryl acrylate as monomer not capable of hydrogen bonding. The results of the experiments with undecyl amide *N*-ethyl acrylate are shown in Figure 4.

The temperature-dependent behavior of lauryl acrylate, which corresponded to an activation energy around 4–5 kJ/mol, is in good agreement with the values obtained using photo-DSC.^{2a,c} For diacrylates, using RT-IR up to 90 °C a similar activation energy has been found.²³ Therefore, the behavior of undecyl amide *N*-ethyl acrylate clearly deviates from the Arrhenius behavior of normal acrylates.

Since we are employing RT-FTIR, we are able to monitor simultaneously the amide shifts as well as the acrylate conversions. The amide II bond shifts from 1546 cm^{-1} at 30 °C to 1539 cm^{-1} at 90 °C, and the N–H shifts from 3312 cm^{-1} at 30 °C to 3325 cm^{-1} at 90 °C. Both shifts are indicative of reduced hydrogen bonding at elevated temperatures. Unfortunately, the quantitative extent of hydrogen bonding at 30 or 90 °C is unknown; therefore, it is difficult to proportionate the extent of hydrogen bonding with R_p . It should be noted that with urethane and urea acrylates we were only able to observe a clear IR spectral shift toward non-hydrogen bonding at higher temperatures with the corresponding N–H absorptions.

This reduction in R_p , at elevated temperatures, combined with the observed IR shifts, provides additional evidence validating the fact that hydrogen bonding is a key issue in these rate enhancements. However, this

Scheme 2. Proposed Mechanism by Which Preorganization via Hydrogen Bonding Could Lead to the Formation of Isotactic Polymer

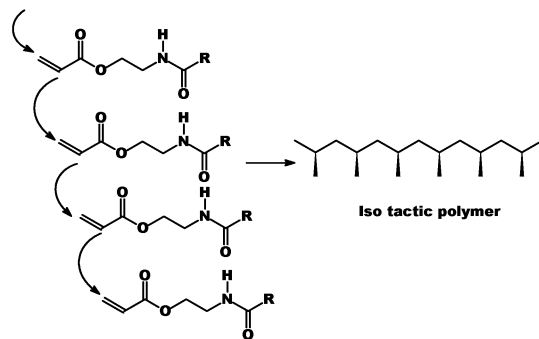


Table 2. Tacticity of Polymethacrylates, Based on ^{13}C NMR, Formed by Photoinitiated Polymerization

tacticity (%)	undecyl amide <i>N</i> -ethyl-methacrylate (29)	pentyl amide <i>N</i> -methyl <i>N</i> -ethyl-methacrylate (30)	lauryl methacrylate
syndio	58	65	65
a	28	33	31
iso	14	2	4

anti-Arrhenius behavior cannot discriminate between the two different theories.

Effect on Tacticity. The effect of preorganization can be examined further by looking at the tacticity of the resultant polymer. Only in case where intermolecular preorganization via hydrogen bonding is significant can an effect on the resultant polymer tacticity can be expected. Generally, polyacrylates produced by a free radical mechanism yield predominantly syndiotactic material. However if we assume that the polymerization proceeds via an organized structure, then isotactic polyacrylate can be envisaged as shown in Scheme 2.

However, it is unlikely that all the monomers will be fully preorganized in order to give pure isotactic polymer. Experiments were performed in order to see if there was enhanced isotacticity in the resultant polymers. Since the tacticity can be better determined with methacrylates instead of acrylates, the experiments to determine tacticity were performed with the following methacrylates: undecyl amide *N*-ethyl methacrylate **29** as monomer capable of hydrogen bonding, pentyl amide *N*-methyl *N*-ethyl methacrylate **30** as control compound possessing the amide functionality but incapable of hydrogen bonding, and lauryl methacrylate as reference sample. The results are shown in Table 2.

The tacticity of poly(lauryl methacrylate) (polyLMA) produced via photoinitiated polymerization is identical to polyLMA prepared with thermal initiators like AIBN, thereby eliminating a possible effect due to the initiator employed.²⁴ The tacticity of poly(pentyl amide *N*-methyl *N*-ethyl methacrylate) is the same as for polyLMA (within the errors of the measurements). This strongly indicates that an amide function itself does not alter the tacticity of the polymer. Analyzing the poly(undecyl amide *N*-ethyl methacrylate) formed we observed an increased amount of isotactic triads as determined by NMR. This enhancement is significant and beyond the instrumental and experimental errors. The enhanced isotacticity observed with hydrogen-bonding acrylates suggests that preorganization via intermolecular hydrogen bonding plays a dominant role in how the acrylates groups are oriented toward each other. Therefore, this provides additional evidence for the hydrogen-

bonding-assisted preorganization, its effects on the R_p , and the tacticity of resultant polymer.

Although all the data presented above suggest that hydrogen bonding affects the propagation rate constant and not the termination constant, the ultimate proof obviously is the determination of the kinetic constants. It is difficult to obtain a correct comparison, a difference in hydrogen bonding but no difference in dipole moment (see below) for the determination of the rate constants, although the first results indicate that indeed k_p is affected and not k_t . This item will be discussed further when the effects of polarity and hydrogen bonding are combined.

Monomers Not Capable of Hydrogen Bonding.

As mentioned in the Introduction (Figure 2), other monomers with enhanced reactivity exist for which the hydrogen-bonding theory offers no explanation since these monomers are not capable of forming hydrogen bonds. Therefore, another mechanism that explains the high reactivity of non-hydrogen-bonding monomers has to be considered. Decker¹¹ and Bowman²⁵ both mention hydrogen abstraction reactions, via which cross-links can be introduced, as the explanation for the high reactivity. The cross-links could lead to a viscosity increase,²⁶ earlier start of gelation, thereby allowing an earlier onset of autoacceleration (Trommsdorf effect²⁷), which would account for high R_p 's. However, experimental evidence, in the literature, is inconclusive. The fact that the polymerization of glycerol carbonate acrylate **57** can be initiated with benzophenone, a Norrish type II photoinitiator, suggests that under these conditions some of the hydrogens are relatively labile. However, it does not indicate that these hydrogens are abstracted during the radical polymerization. It only demonstrates that they can be abstracted during the initiation (when nothing else can happen). The other feature, which is assumed to prove the cross-link hypothesis, is the formation of gel particles. Again, this only proves that some of the hydrogen atoms can be abstracted. In fact, polymerizing lauryl acrylate with a very high UV dose will result in the formation of gel particles. Moreover, butyl acrylate polymerized at 60 °C will also give some gel particles.¹⁷ The experimental data, which suggest that hydrogen abstraction is not the mechanistic pathway, is not discussed in these papers. The fact that the oxazolidone functional acrylate **56** has a lower R_p compared to that of glycerol carbonate acrylate **57** is ignored in the discussions. A consequence of the hydrogen abstraction theory would be that the oxazolidone functional acrylate **56**, possessing more and more labile hydrogens (adjacent to a nitrogen atom instead of an oxygen atom), should react faster than the glycerol carbonate acrylate **57**. On the contrary, the oxazolidone functional acrylate **56** has a lower R_p compared to that of the glycerol carbonate functional acrylate **57**. In light of our results and often contradictory reports on the effect of hydrogen abstraction, we decided to explore whether dipolar interactions could account for the high intrinsic polymerization reactivity of certain acrylates, especially since it is well-known that polarity is important in radical addition reactions.^{28,29} Tedder²⁹ postulated a second law of free radical reactions based on polarity effects.

The main problem faced in any attempt to discuss or experimentally determine acrylate reactivity in terms of dipolar interactions is the fact that for most of the interesting reactive monomers neither the dipole mo-

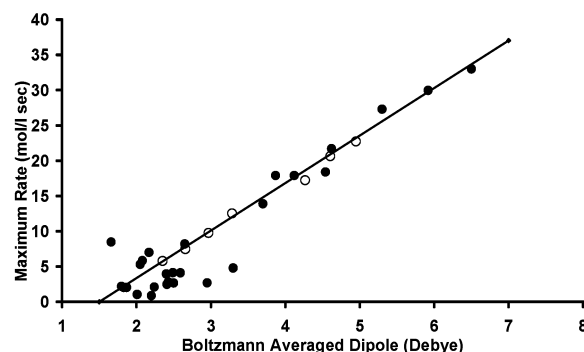
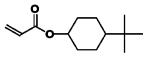
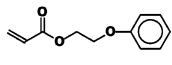
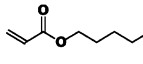
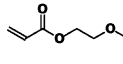
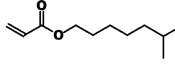
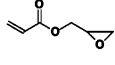
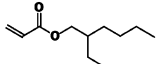
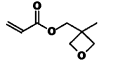
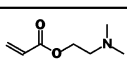
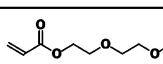
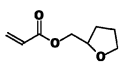
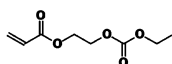
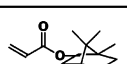
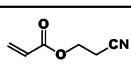
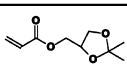
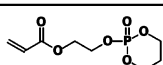
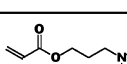
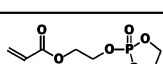
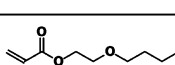
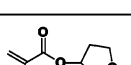

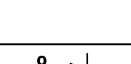
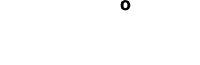
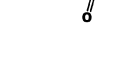
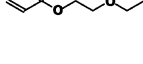
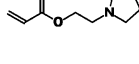
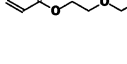
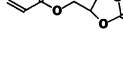


Figure 5. Correlation between the calculated Boltzmann-averaged dipole moment and the maximum rate of photoinitiated polymerization as determined with RT-FTIR. Closed circles, neat monomers; open circles, mixtures of monomers.

ments nor the dielectric constants are known. Although the calculated dipole moment of an energy-minimized structure could give an indicative value, it has to be realized that in a (neat) solution more conformations than only the minimum-energy structure are present and that the average dipole moment could therefore differ significantly from the dipole of the energy-minimized structure. Acknowledging this, we calculated the dipole moments as the Boltzmann-averaged dipole moments (μ_{calc}), and we believe that the Boltzmann-averaged dipole moment is a good representation of dipole of a neat solution. As far as we are aware, this is the first time that dipole moments are calculated as Boltzmann-averaged dipole moments. Normally, the dipole moment of the global energy-minimized structure is used (μ_{gm}). The following series is illustrative for the large differences which can be found employing these two methods: compound **36**: $\mu_{\text{calc}} = 2.05$ D, $\mu_{\text{gm}} = 1.74$ D; compound **38**: $\mu_{\text{calc}} = 2.17$ D, $\mu_{\text{gm}} = 2.28$ D; compound **48**: $\mu_{\text{calc}} = 2.65$ D, $\mu_{\text{gm}} = 3.50$ D; compound **49**: $\mu_{\text{calc}} = 2.93$ D, $\mu_{\text{gm}} = 3.2$ D; compound **56**: $\mu_{\text{calc}} = 5.3$ D, $\mu_{\text{gm}} = 4.9$ D; compound **57**: $\mu_{\text{calc}} = 5.9$ D, $\mu_{\text{gm}} = 6.6$ D. The differences employing monomers not capable of hydrogen bonding are still minor compared to monomers capable of hydrogen bonding: compound **1**: $\mu_{\text{calc}} = 4.31$ D, $\mu_{\text{gm}} = 2.83$ D; compound **5**: $\mu_{\text{calc}} = 3.24$ D, $\mu_{\text{gm}} = 0.93$ D; compound **9**: $\mu_{\text{calc}} = 3.23$ D, $\mu_{\text{gm}} = 2.11$ D; compound **13**: $\mu_{\text{calc}} = 4.64$ D, $\mu_{\text{gm}} = 2.6$ D; compound **21**: $\mu_{\text{calc}} = 3.3$ D, $\mu_{\text{gm}} = 1.83$ D. Especially the fact that compounds **5** and **9** possess almost the same R_p as well as the same (μ_{calc}) but a very different μ_{gm} corroborates our belief that calculating Boltzmann-averaged dipole moments is the correct procedure.

After some initial experiments in which we applied the calculated dipole moments of the global energy-minimized structure, we realized that there could be a direct correlation between the dipole moment and the R_p and that the observed deviations might be due to the incorrect method of calculating the dipole moment. Only after this realization we started the calculations of the Boltzmann-averaged dipole moments, instead of the global energy-minimized dipole moments, for a large set of monomers and compared them to the R_p values. The results of this study are shown in Table 3 and Figure 5 (black circles). The results clearly show that for monomers with calculated dipole moments (μ_{calc}) above 3.5 D there is a direct correlation between the R_p and (μ_{calc}). This correlation between a monomer molecular structure, its associated polarity, and R_p for acrylate polymerization enables the rational design of new monomers

Table 3. Maximum Rates (mol/(L s)) of Photoinitiated Polymerization of Monomers Not Capable of Capable of Hydrogen Bonding As Measured by RT-FTIR Using a Transflection Cell at Room Temperature Employing a Light Intensity of 135 mW/cm² (Medium-Pressure Mercury Lamp) and Their Calculated Boltzmann-Averaged Dipole Moments

no	Structure	Dipole (Debye)	Rate (mol/l sec)	no	Structure	Dipole (Debye)	Rate (mol/l sec)
31		1.66	8.47	45		2.49	4.12
32		1.8	2.2	46		2.5	2.67
33		1.83	2.04	47		2.59	4.11
34		1.87	2.04	48		2.65	8.2
35		2.01	1.04	49		2.95	2.7
36		2.05	5.3	50		3.3	4.79
37		2.08	5.83	51		3.7	13.9
38		2.17	7	52		3.87	17.9
39		2.2	0.88	53		4.12	17.9
40		2.24	2.1	54		4.54	18.4
41		2.4	3.95	55		4.62	21.7
42		2.41	2.47	56		5.3	27.3
43		2.42	2.67	57		5.92	30
44		2.43	2.82	58		6.5	33

with a designed reactivity instead of the trial-and-error strategies applied so far.

Thus, a direct correlation with (μ_{calc}) and R_p has been found. So the *averaged* dipole moment is determining

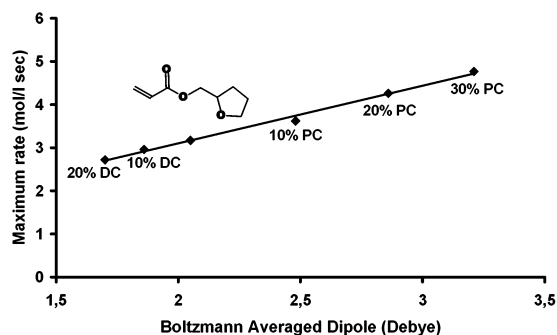


Figure 6. Correlation between the calculated Boltzmann-averaged dipole moment and the maximum rate of photoinitiated polymerization of tetrahydrofurfuryl acrylate diluted with dimethyl carbonate (DC) or propylene carbonate (PC) as determined with RT-FTIR.

the maximum rate of polymerization. These results open up two possibilities. The first is that under identical conditions mixtures of acrylates should obey the same correlation. The second is that in case small amounts of highly polar inert solvents are added the rates of polymerization should increase.

To evaluate the first possibility, we examined the photoinitiated polymerization of various mixtures of tetrahydrofurfuryl acrylate **36** ($\mu_{\text{calc}} = 2.05$ D) and oxazolidone-*N*-ethyl acrylate **56** ($\mu_{\text{calc}} = 5.3$ D). The results were in line with the $\mu_{\text{calc}}-R_p$ correlation and are shown in Figure 5 (open circles). These findings demonstrate that the $\mu_{\text{calc}}-R_p$ correlation is valid for mixtures of monomers as well as neat monomers.

The second possibility takes this theory one step further as it suggests that rate enhancements can be achieved by the addition of polar inert solvents, which is contradictory to the general belief that dilution with an inert solvent automatically will lead to a reduction of the polymerization rate (due to the reduced monomer concentration). To examine the role of the solvent, we diluted tetrahydrofurfuryl acrylate **36** with a high polar (propylene carbonate, $D = 5$ D) and with a low polar (dimethyl carbonate, $D = 0.9$ D) solvent. RT-FTIR experiments on the diluted samples seek to determine whether the $\mu_{\text{calc}}-R_p$ relationship can be exploited using polar solvents. In Figure 6 the results of these experiments using laminates, to avoid evaporation of the solvents, are shown. Unfortunately, the use of a laminated experimental setup results in different light intensity and sample thickness compared to the previous experiments with the transmission-reflection setup. These changes result in different R_p values and as a consequence a different correlation. However, the basic $\mu_{\text{calc}}-R_p$ relation remains intact. The R_p values of neat tetrahydrofurfuryl acrylate **36** are indicative for the changes in experimental setup as a R_p of 5.3 mol/(L s) is found in the transmission reflection setup whereas a R_p of 3 mol/(L s) in the transmission setup using laminates. It should be noted that the correlation found in the dilution experiments with inert solvents is only valid as long as the bulk of the solution is the acrylate monomer (up to 30% inert solvents). Still this feature demonstrates that polymerization rate enhancements via the addition of small amounts of an inert solvent can be achieved contrary to the general belief that dilution automatically leads to reductions in polymerization rates.^{30,31}

In summary, we have demonstrated that a direct correlation exists between the Boltzmann-averaged

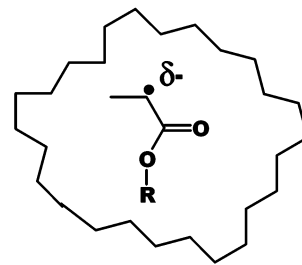


Figure 7. Illustration of the propagating radical envisaging the solvent cage and the enhanced charging of the propagating radical.

dipole moment (μ_{calc}) and the maximum rate of polymerization (R_p) for monomers not capable of hydrogen bonding, and this offers a tool for the rational design of inherently reactive monomers.

Mechanism? Several possible explanations for this relationship can be envisaged: (a) The photoinitiator can be more effective in a more polar medium.³² As more initiating radicals are generated in this way a higher rate of polymerization will be found. (b) The activation energy of propagation can be reduced in a more polar medium, leading to a faster propagation reaction. (c) Hydrogen abstraction reactions leading to cross-link points are facilitated; therefore, an earlier onset of autoacceleration may occur. (d) A stronger solvent cage around the propagating radical is formed in a higher polarity medium, resulting in a lower termination reaction rate and consequently faster polymerization.³³ (e) In a higher dipole medium, the propagating radical is charged to a greater extent, resulting, due to the increased electrostatic repulsion between the terminating radicals, in a reduction of the termination reaction rate.³⁴

None of these possible explanations can be ruled out so far. However, there is experimental evidence that makes some explanations less plausible.

The activation energy of polymerization of some acrylates has been determined using photo-DSC or RT-FTIR.^{2a,c} In the temperature range 30–90 °C the maximum activation energy found is only 5 kJ/mol. Such a low value suggests that the reaction could be diffusion-controlled. Consequently, changes in activation energy would only have a minor effect on the rate-limiting process. Therefore, it seems unlikely that further reduction of such a low value would be the cause of the rate increase observed above. However, it should be noted that according to pulsed laser experiments at low temperatures (range –60 to 20 °C) the energy of activation is higher than the above-mentioned 5 kJ/mol, namely around 17 kJ/mol for the acrylates studied by PLP. Still, even in this case the activation energy is relatively low.³⁵

As mentioned above in the introduction to this section, the hydrogen abstraction theory offers no explanation why the oxazolidone functional acrylate **56** is less reactive compared to the glycerol carbonate functional acrylate **57**. The formation of a stronger solvent cage around the propagating radical can explain the experimental evidence so far, especially the rate polymerization increase using small amounts of inert solvent. Furthermore, this theory explains why the solvent effect as shown in Figure 7 is only valid for low amounts of inert solvent. The formation of a stronger solvent cage may reduce the probability of termination (lower k_t) but normally could reduce the probability of propagation as

well (lower k_p). As the solvent cage is mainly based on the acrylate monomer, this negative effect on k_p will be negligible in these dilution experiments using small amounts of inert solvents, whereas the positive effect on k_t is still present. The reduction in k_p at higher dilutions, as well as the concentration effect, can overcome the positive effect of the reduction in k_t , which eventually could lead to lower polymerization rates employing higher dipolar solvents, obscuring the dipole effects in diluted polymerizations.³⁶ However, it should be noted that, on the basis of pulsed laser experiments, solvent effects on k_p are generally small.³⁷

A solvent cage around the propagating radical has been suggested in order to explain the experimental results in vinyl polymerizations.³⁸ With aromatic solvents the formation of complexes between the propagating radical and the solvent has been proposed.³⁹ On the basis of such a complex a kinetic model, the so-called "reactant-solvent complex model (RSC)" has been postulated.⁴⁰

Molecular modeling calculations employing ESP charge calculations revealed that in a high-polarity medium the propagating radical (simulated by the methyl propionate radical in a field with a fixed dielectric constant) is negatively charged to a greater extent relative to the charge in a low-polarity medium. This is demonstrated with the following series: dimethyl carbonate $D = 0.9$ D, charge -0.2049 ; ethylene carbonate $D = 5$ D, charge -0.2207 . Although these calculations have not been performed at the most refined level, they still give some credibility to this theory.

It is our belief that a combination of the latter two explanations is what really occurs, as depicted in Figure 7. A stronger solvent cage and an enhanced radical charge may be formed in a highly polar medium, and this may account for enhanced reactivity. Further experiments to determine the effect of solvent polarity on the polymerization initiation (k_i), propagation (k_p), and termination (k_t) rate constants are required.

It should be noted that such a solvent cage or radical-solvent complex is required for the elucidation of the solvent effects on radical hydrogen abstraction reactions. On the basis of the solvent cage theory, a good explanation for the fact that the rates of hydrogen abstraction are independent of the nature of the abstracting radical is given.⁴¹ A prediction of the solvent effect on the rate of hydrogen abstraction based on Abrahams parameters, which describe the hydrogen-donating and hydrogen-accepting abilities is possible.⁴² Furthermore, solvent cage effects are frequently mentioned as explanation of solvent effects on radical copolymerizations.⁴³

This solvent cage enhanced charging explanation of the $\mu_{\text{calc}}-R_p$ correlation has some consequences, which we can explore further. First the k_p 's of a high and low polarity monomer should be similar whereas a significant difference in k_t should exist. Second and more importantly, the hydrogen-bonding mechanism and the dipole theory should be complementary.

Employing the methodology as described by Decker,¹¹ the kinetic parameters of tetrahydrofurfuryl acrylate **36** and lactone acrylate **54** were determined (see Table 4). The values for the k_p 's and k_t 's at R_p were in line with our expectations. Similar propagation rate constants (k_p) were found. The termination rate constants (k_t), however, showed a significant difference of almost 2 orders of magnitude. These observations are comparable with

Table 4. Kinetic Parameters at R_p of Selected Monomers

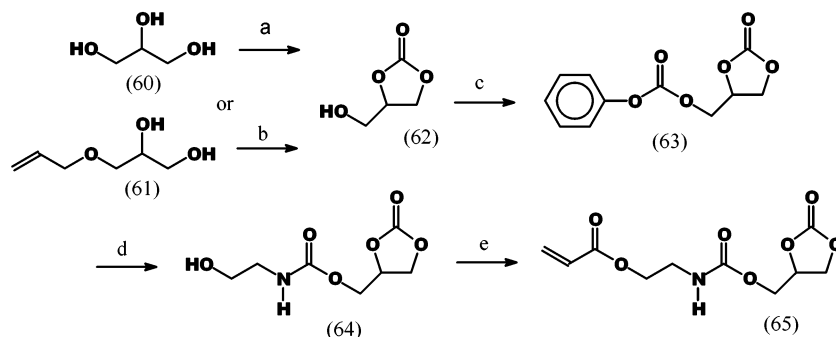
compound	μ_{calc}	k_p	k_t
36	2.05	8×10^3	1.2×10^6
HEA	2.93	1.5×10^4	7×10^5
54	4.54	7×10^3	7×10^4

the data presented by Decker, who found similar k_p 's but significantly different k_t 's as well.

Combining Preorganization via Hydrogen Bonding and the Dipole Theory. A significant consequence of the fundamental explanation behind the dipole theory implies that preorganization via hydrogen bonding and the dipole theory can be combined and are complementary. In fact, it means that monomers capable of hydrogen bonding should possess a higher polymerization rate compared to monomers with the same dipole moment but without hydrogen-bonding capability. Moreover, if the hydrogen-bonding effect can fully be attributed to a change in k_p , then a similar increase in R_p as a function of polarity should be found for hydrogen-bonding monomers as well as non-hydrogen-bonding monomers; i.e., in Figure 5 they should be on a parallel line, with for the same dipole moment a higher rate. The Boltzmann-averaged dipole moments for several acrylate monomers capable of hydrogen bonding were calculated [ethyl-substituted amide rate **1** 23.5 mol/(L s), 4.31 D; urethane **5** rate 16.1 mol/(L s), 3.24 D; "inverted" urethane **9** rate 15.9 mol/(L s), 3.23 D; and urea rate 25.2 mol/(L s), 4.64 D functional ethyl acrylates **13** and hydroxyethyl acrylate HEA, rate 14 mol/(L s), 2.93 D].

At first glance, this complementarity seems to hold. However, the range of calculated dipole moments of these monomers is rather limited and varies only from 3 to 4.5 D. A suitable monomer capable of hydrogen bonding and with a very high dipole moment is lacking. On the basis of our knowledge gained previously, we expected that the five-ring cyclic carbonate urethane ethyl acrylate (synthesis is shown in Scheme 3) would possess a very high Boltzmann-averaged dipole moment. A μ_{calc} of 7.5 D was obtained. Because of this very high value, we reconsidered our method of calculating dipole moments, especially since lithium chloride has a value around 9 D.

To validate our method of calculation, employing the semiempirical AM1 method, we compared the calculated Boltzmann-averaged dipole moments of ethylene carbonate, γ -butyrolactone, dimethyl carbonate, ethyl propionate, methacrylic acid, methyl methacrylate, *n*-propyl methacrylate, and *n*-butyl methacrylate with experimental values found in the literature. Moreover, we also compared them with dipole moments calculated using other advanced calculation methods. The first-principle methods, which were employed, involved Hartree-Fock (HF), density functional (BLYP and BPW91), HF-DFT hybrid methods (B3LYP and B3PW91), and second-order Møller-Plesset perturbation theory (MP2). For the optimizations at the HF, MP2, BLYP, BPW91, B3PW91, and B3LYP-level the 6-31G* basis sets were employed. In addition, using the BLYP and MP2 method, the effect of the basis set size was investigated. For γ -butyrolactone and dimethyl carbonate geometry optimizations were also performed using the larger 6-31G** and 6-311G** basis sets, and single-point calculations on the 6-31G* geometries were carried out using the 6-31G**, 6-311G**, 6-311++G**, and 6-311+G(3df,2p) basis sets. Although the validation

Scheme 3. Synthesis of Glycidyl Carbonate Urethane Acrylate **65**^a

^a Reagents: (a) ethylene carbonate, NaOH; (b) COCl₂, Et₃N followed by Pd/C; (c) phenylchloroformate, Et₃N, 0 °C; (d) ethanamine, −5 °C; (e) acryloyl chloride, pyridine, 0 °C.

of our calculational method was slightly hampered by the scatter in the literature data (± 0.2 D), it showed that our method of calculating the Boltzmann-averaged dipole moment employing AM1 performs well.

After having confirmed the method of calculating, we embarked on the synthesis of the five-ring cyclic carbonate urethane ethyl acrylate as this possesses μ_{calc} of 7.5 D. Although 2-isocyanatoethyl acrylate might seem the ideal precursor for this molecule, we were unable to prepare this acrylate. Therefore, as alternative to using 2-isocyanatoethyl acrylate, we employed the synthetic procedure shown in Scheme 3.

Glycerol carbonate was prepared in two ways. The standard procedure starting from glycerol **60** and reacting with ethylene carbonate yields glycerol carbonate **62**. However, this product still contains some glycerol and higher oligomers, which are very difficult to remove by distillation. Therefore, to obtain glycerol carbonate **62** without traces of glycerol, the synthesis started from monoallyl-protected glycerol **61**. Phosgene as well as the less toxic di- and triphosgene can be used for the carbonate formation, and after removal of the allyl protecting group pure glycerol carbonate can be obtained in 56% yield over two reaction steps. Next, the glycerol carbonate was reacted with phenyl chloroformate, yielding the active ester **63**. The choice of active ester is crucial for the success of the next reaction step. The acidity of the liberated phenol should be as low as possible. In this way the subsequent reaction can be performed without the addition of base, which besides neutralizing the liberated acid also enhanced the nucleophilicity of the amine, thereby leading to side reactions. In those cases where a tertiary amine like triethylamine or pyridine was added, we noticed some reaction on the cyclic carbonate yielding unwanted side products. It should be noted that the hydroxy functional urethane carbonate **64** is very polar and dissolves readily in water. On the basis of alcohol **64** the synthesis of glycidyl carbonate urethane acrylate **65** is straightforward, and the product can be obtained pure (starting from **61**) in a calculated 6% overall yield over five reaction steps. In case lower purities can be tolerated, obviously much higher yields can be obtained as distilling **65** results in large product losses. Alongside this synthesis, we used the commercially available 2-isocyanatoethyl methacrylate and glycidyl carbonate for the preparation of the methacrylate analogue to **65**.

Unfortunately, the five-ring cyclic carbonate urethane ethyl acrylate **65** was a solid at room temperature. Consequently, the maximum rate (38 mol/(L s)) was determined at 50 °C. Since at higher temperatures the

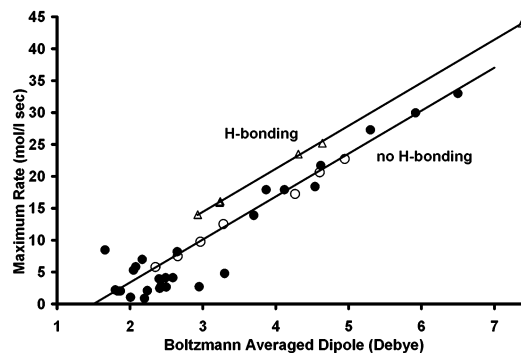


Figure 8. Correlation between the μ_{calc} and R_p as determined with RT-FTIR. Closed circles, neat monomers; open circles, mixtures of monomers; open triangles, monomers capable of hydrogen bonding.

level of hydrogen bonding is reduced, a higher rate is expected at room temperature. Acknowledging the $\mu_{\text{calc}}-R_p$ relationship, a R_p of 44 mol/(L s) was predicted. In line with this prediction, a R_p of 43.5 mol/L was based on extrapolation from the methacrylate analogue. The combined $\mu_{\text{calc}}-R_p$ plot using all the evaluated monomers is shown in Figure 8.

The scatter in R_p at low μ_{calc} values (< 3.5 D) might be due to other effects. These effects could be for instance polymer T_g , molecular packing phenomena due to van der Waals interactions, or even hydrogen abstraction reactions, retarding the polymerization. However, it is evident that for values above 3.5 D the $\mu_{\text{calc}}-R_p$ relationship is valid. Moreover, monomers capable of both hydrogen bonding and having a high μ_{calc} appear to obey a similar relationship at the expected higher polymerization rates.

The simple fact that the correlation coefficients are the same, as illustrated with parallel lines in Figure 8 is a strong indication that both effects operate via different mechanisms. The proposed effect on k_p of hydrogen bonding and the proposed effect on k_t due to the dipole moment are in line with this reasoning.

However, so far all the experimental evidence are only strong indications. The final proof is measuring the actual kinetic constants. In Table 4 the kinetic data from two monomers not capable of hydrogen bonding, i.e., **36** and **54** and a monomer capable of hydrogen bonding HEA at R_p are given. The trends in k_t are clearly in line with the proposed effect of the dipole moment on the termination rate. At higher dipole moments lower values for k_t are found. The fact that hydrogen bonding affects k_p is nicely illustrated by the double value of k_p of HEA compared to **36** and **54**. So the kinetic analysis

corroborate the theories presented here: hydrogen bonding causes rate enhancement by increasing k_p , and a higher dipole moment causes a rate enhancement by decreasing k_t .

Conclusion

In conclusion, we have given evidence that R_p is dominated by two molecular factors: hydrogen bonding and the Boltzmann-averaged dipole moment, which are complementary to each other. Hydrogen bonding affects R_p via preorganization of the monomers whereas the Boltzmann-averaged dipole moment (μ_{calc}) may affect R_p due to a stronger solvent cage combined with increased charge at the propagating radical. This understanding of acrylate reactivity at the molecular level enables the rational design of monomers with a defined reactivity as opposed to the trial-and-error strategy applied so far. Moreover, the effect of the addition of small amounts of polar solvents on R_p is demonstrated and could prove useful in practical systems. In fact, solvents can be used to enhance the reactivity of the acrylate monomers.

Acknowledgment. The management of DSM Research, DSM Coating Resins, and DSM Desotech are kindly acknowledged for their permission to publish this work.

References and Notes

- (1) (a) Nie, J.; Rabek, J. F.; Linden, L.-A. *Polym. Int.* **1999**, *48*, 129. (b) Narayanan, V.; Scranton, A. B. *Trends Polym. Sci.* **1997**, *5*, 415. (c) Lovell, L. G.; Stansbury, J. W.; Sympes, D. C.; Bowman, C. N. *Macromolecules* **1999**, *32*, 3913 and references therein. (d) Kloosterboer, J. G. *Adv. Polym. Sci.* **1988**, *84*, 1.
- (2) (a) Tryson, G. R.; Schultz, A. R. *J. Polym. Sci., Polym. Phys. Ed.* **1979**, *17*, 2059. (b) Decker, C.; Elzaouk, B.; Decker, D. *J. Macromol. Sci., Pure Appl. Chem.* **1996**, *A33*, 173 and references therein. (c) Doornkamp, A. T.; Tan, Y. Y. *Polym. Commun.* **1990**, *31*, 362. (d) Lecamp, L.; Youssef, B.; Bunel, C.; Lebaudy, P. *Polymer* **1999**, *40*, 1403. (e) Khudyakov, I. V.; Legg, J. C.; Purvis, M. M.; Overton, B. J. *Ind. Eng. Chem. Res.* **1999**, *38*, 3353. (f) Selli, E.; Bellobono, I. R. In *Radiation Curing in Polymer Science and Technology*; Fouassier, J. P.; Rabek, J. F., Eds.; Elsevier: London, Vol. 3, p 1. (g) Decker, C.; Masson, F.; Bianchi, C. *Polym. Prepr.* **2001**, *42*, 304. (h) Yamada, B.; Azukizawa, M.; Yamazoe, H.; Hill, D. J. T.; Pomery, P. J. *Polymer* **2000**, *41*, 5611. (i) Seno, M.; Fukui, T.; Hirano, T.; Sato, T. *J. Polym. Sci., Part A: Polym. Chem.* **2000**, *38*, 4264. (j) Doetschman, D. C.; Mehlenbach, R. C.; Cywar, D. *Macromolecules* **1996**, *29*, 1807.
- (3) (a) Anseth, K. S.; Bowman, C. N. *Polym. React. Eng.* **1993**, *1*, 499. (b) Anseth, K. S.; Wang, C. M.; Bowman, C. N. *Macromolecules* **1994**, *27*, 650. (c) Young, J. S.; Bowman, C. N. *Macromolecules* **1999**, *32*, 6073.
- (4) Wen, M.; McCormick, A. V. *Macromolecules* **2000**, *33*, 9247.
- (5) Goodner, M. D.; Bowman, C. N. *Macromolecules* **1999**, *32*, 6552.
- (6) Berchtold, K. A.; Hacıoglu, B.; Lovell, L. G.; Nie, J.; Bowman, C. N. *Macromolecules* **2001**, *34*, 5103.
- (7) (a) Hutchinson, J. B.; Anseth, K. S. *Polym. Prepr.* **2000**, *41*, 1326. (b) Lu, H.; Lovell, L. G.; Bowman, C. N. *Macromolecules* **2001**, *34*, 8021.
- (8) (a) Elliot, J. E.; Bowman, C. N. *Macromolecules* **1999**, *32*, 8621. (b) Elliot, B. J.; Willis, W. B.; Bowman, C. N. *Macromolecules* **1999**, *32*, 3201. (c) Elliot, B. J.; Scranton, A. B.; Cameron, J. H.; Bowman, C. N. *Chem. Mater.* **2000**, *12*, 633.
- (9) (a) Elliot, J. E.; Bowman, C. N. *Macromolecules* **2001**, *34*, 4642. (b) Lovell, L. G.; Stansbury, J. W.; Sympes, D. C.; Bowman, C. N. *Macromolecules* **1999**, *32*, 3913.
- (10) Berchtold, K. A.; Lovell, L. G.; Nie, J.; Hacıoglu, B.; Bowman, C. N. *Polymer* **2001**, *42*, 492 and references therein.
- (11) (a) Decker, C.; Moussa, K. *Polym. Mater. Sci. Eng.* **1989**, *60*, 547. (b) Decker, C.; Moussa, K. *Makromol. Chem. Rapid Commun.* **1990**, *11*, 159. (c) Decker, C.; Moussa, K. *Makromol. Chem.* **1990**, *192*, 507. (d) Decker, C.; Moussa, K. *Eur. Polym. J.* **1991**, *27*, 403. (e) Decker, C.; Moussa, K. *Eur. Polym. J.* **1991**, *27*, 881. (f) Moussa, K.; Decker, C. *J. Polym. Sci., Part A: Polym. Chem.* **1993**, *31*, 2197. (g) Decker, C.; Elzaouk, B. *Eur. Polym. J.* **1995**, *31*, 1155. (h) Decker, C.; Elzaouk, B.; Decker, D. *J. Macromol. Sci., Pure Appl. Chem.* **1996**, *A33*, 173.
- (12) Andrzejewska, E.; Andrzejewski, M. *J. Polym. Sci., Part A: Polym. Chem.* **1998**, *36*, 665.
- (13) (a) Guymon, C. A.; Hoggan, E. N.; Clark, N. A.; Rieker, T. P.; Walba, D. M.; Bowman, C. N. *Science* **1997**, *275*, 57. (b) Guymon, C. A.; Bowman, C. N. *Macromolecules* **1997**, *30*, 5271. (c) Lester, C. L.; Colson, C. D.; Guymon, C. A. *Macromolecules* **2001**, *34*, 4430.
- (14) (a) Jansen, J. F. G. A.; Dias, A. A.; Dorsch, M.; Coussens, B. *Polym. Prepr.* **2001**, *42*, 769. (b) Jansen, J. F. G. A.; Dias, A. A.; Dorsch, M.; Coussens, B. *Macromolecules* **2002**, *35*, 7529. (c) Jansen, J. F. G. A.; Dias, A. A.; Dorsch, M.; Coussens, B. Patent WO 02/42383.
- (15) Dias, A. A.; Hartwig, H.; Jansen, J. F. G. A. *Surf. Coat. Int., JOCCA* **2000**, *83*, 382.
- (16) (a) Decker, C.; Moussa, K. *Polym. Prepr.* **1988**, *29*, 516. (b) Decker, C.; Moussa, K. *Makromol. Chem.* **1988**, *189*, 2381. (c) Decker, C.; Moussa, K. *Eur. Polym. J.* **1990**, *26*, 393. (d) Decker, C.; Moussa, K. *Makromol. Chem.* **1990**, *191*, 963. (e) Decker, C. *Macromolecules* **1990**, *23*, 5217. (f) Decker, C.; Moussa, K. *J. Coat. Technol.* **1990**, *62*, 55. (g) Decker, C. *J. Polym. Sci., Part A: Polym. Chem.* **1992**, *30*, 913. (h) Decker, C. *Spec. Publ.-R. Soc. Chem.* **1993**, *125*, 32 and refs 11g and 11h.
- (17) The formation of gel particles in butyl acrylate has been described in: Plessis, C.; Arzamendi, G.; Leiza, J. R.; Schoonbrood, H. A. S.; Charmont, D.; AUSA, J. M. *Macromolecules* **2000**, *33*, 4.
- (18) (a) Computational results obtained using software programs from Molecular Simulations force field calculations were done with the Discover program, using the CVFF force-field, semiempirical calculations were done with the MOPAC 6.0 program. (b) Frisch, M. J.; Trucks, G. W.; Schlegel, H. B.; Scuseria, G. E.; Robb, M. A.; Cheeseman, J. R.; Zakrzewski, V. G.; Montgomery, J. A., Jr.; Stratmann, R. E.; Burant, J. C.; Draprich, S.; Millam, J. M.; Daniels, A. D.; Kudin, K. N.; Strain, M. C.; Farkas, O.; Tomasi, J.; Barone, V.; Cossi, M.; Cammi, R.; Mennucci, B.; Pomelli, C.; Adamo, C.; Clifford, S.; Ochterski, J.; Petersson, G. A.; Ayala, P. Y.; Cui, Q.; Morokuma, K.; Malick, D. K.; Rabuck, A. D.; Raghavachari, K.; Foresman, J. B.; Cioslowski, J.; Ortiz, J. V.; Stefanov, B. B.; Liu, G.; Liashenko, A.; Piskorz, P.; Komaromi, I.; Gomperts, R.; Martin, R. L.; Fox, D. J.; Keith, T.; Al-Laham, M. A.; Peng, C. Y.; Nanayakkara, A.; Gonzalez, C.; Challacombe, M.; Gill, P. M. W.; Johnson, B.; Chen, W.; Wong, M. W.; Andres, J. L.; Gonzalez, C.; Head-Gordon, M.; Replogle, E. S.; Pople, J. A. *Gaussian 98*, revision A.5; Gaussian, Inc.: Pittsburgh, PA, 1998. See also: Scott, A. P.; Radom, L. *J. Phys. Chem.* **1996**, *100*, 16502.
- (19) The naming of the compounds is according to the following scheme: alkyl group-second functionality-alkylbridge-acrylate. In case of urethanes also the atoms, i.e., N and O, which connects to the alkyl groups are mentioned. Using this naming methodology, the changes in the second functionality can be directly compared with their effect on the rate of polymerization.
- (20) (a) Krimm, H.; Buysch, H.-J. European Patent EP 57360, 1998. (b) Buysch, H.-J.; Fengler, G.; Neumann, K.-H.; Wagner, P. German Patent DE 19625265, 1996. (c) Buysch, H.-J.; Fengler, G.; Neumann, K.-H.; Wagner, P.; Melchior, M.; Hovestadt, W. European Patent EP 0816354, 1996.
- (21) (a) Pelet, S.; Yoo, J.-W.; Mouloungui, Z. *J. High-Resolution Chromatogr.* **1999**, *22*, 276. (b) Mouloungui, Z.; Yoo, J.-W.; Gahen, C.-A.; Gaset, A.; Vermeersch, G. European Patent EP739888, 1996. (c) Kawabata, O.; Tanimoto, F.; Inoue, Y. Japanese Patent JP0600910, 1993. (d) Teles, J.-H.; Rieber, N.; Harder, W. European Patent EP 582201, 1993. (e) Rokichi, G.; Kuran, W.; Pogorzelska-Marciniak, B. *Monatsh. Chem.* **1984**, *115*, 205. (f) Rokichi, G.; Kuran, W. *Bull. Chem. Soc. Jpn.* **1984**, *57*, 1662.
- (22) Buermann, S.; Paquet, D. A., Jr.; McMinn, J. H.; Hutchinson, R. A. *Macromolecules* **1997**, *30*, 194.
- (23) Scherzer, T.; Decker, U. *Polymer* **2000**, *41*, 7681.
- (24) Pham, Q.-T.; Petiaud, R.; Waton, H.; Llauro, M.-F. *Proton and Carbon NMR Spectra of Polymers*; J. Wiley & Sons: New York, 1984; Vol 3 and references cited therein.
- (25) Berchtold, K. A.; Nie, J.; Elliot, J. E.; Hacıoglu, B.; Luo, N.; Trotter, A. J. N.; Stansbury, J. W.; Bowman, C. N. *Proc. Radtech Europe* **2001**, 265.

- (26) Employing organogels the R_p of lauryl acrylate was only increased by 15%, although a solid gel was formed. For organogelators see: (a) de Loos, M.; van Esch, J.; Stokroos, I.; Kellogg, R. M.; Feringa, B. L. *J. Am. Chem. Soc.* **1997**, *119*, 12675. (b) van Esch, J.; DeFeyter, S.; Kellogg, R. M.; DeSchrijver, F.; Feringa, B. L. *Chem.—Eur. J.* **1997**, *3*, 1238. (c) de Loos, M.; van Esch, J.; Kellogg, R. M.; Feringa, B. L. *Angew. Chem., Int. Ed.* **2001**, *40*, 613.
- (27) For an excellent review and discussion of the gel effect see: O'Niel, G. A.; Wisnudel, M. B.; Torkelson, J. M. *Macromolecules* **1996**, *29*, 7477.
- (28) Tedder, J. M.; Walton, J. C. *Tetrahedron* **1980**, *36*, 701.
- (29) Tedder, J. M. *Angew. Chem., Int. Ed. Engl.* **1982**, *21*, 401.
- (30) It should be noted that solvent effects in free radical polymerisations are hardly understood. See: *Comprehensive Polymer Science*, Allen, G., Bevington, J. C., Eds.; Pergamon: Oxford, 1989; Vol. 3. For examples of solvent effects in homopolymerizations see: (a) Matyjaszewski, K.; Nakagawa, Y.; Jaszczek, C. B. *Macromolecules* **1998**, *31*, 1535. (b) Couvreur, L.; Piteau, G.; Castignolles, P.; Tonge, M.; Coutin, B.; Charleux, B.; Vairon, J.-P. *Macromol. Symp.* **2001**, *174*, 197. (c) Alvarez, J.; Encinas, M. V.; Lissi, E. *Macromol. Chem. Phys.* **1999**, *200*, 2411. (d) Wang, B.; Xie, S.; Cao, M.; *Chin. J. Polym. Sci.* **1987**, *5*, 141.
- (31) In atom transfer polymerizations a similar effect, i.e., higher rates at a higher solvent polarity has been observed see: (a) Chambard, G.; Klumperman, B.; German, A. L. *Macromolecules* **2000**, *33*, 4417. (b) Kumar Nanda, A.; Matyjaszewski, K. *Macromolecules* **2003**, *36*, 599.
- (32) For solvents effects on initiation see: Turro, N. J.; Kleinman, M. H.; Karatekin, E. *Angew. Chem., Int. Ed.* **2000**, *39*, 4436.
- (33) The effect of a stronger solvent cage on the rate of termination has already been postulated: Mayer, G.; Schultz, G. V. *Makromol. Chem.* **1973**, *173*, 101.
- (34) In radical reactions the ionic nature of the attacking radical is important, See: Citterio, A.; Arnoldi, A.; Minisci, F. *J. Org. Chem.* **1979**, *44*, 2674.
- (35) Using pulsed laser polymerization higher E_a are found. See: van Herk, A. M. *J. Macromol. Sci., Rev. Macromol. Chem. Phys.* **1997**, *C37*, 633.
- (36) Olaj, F. J.; Schnoll-Bitai, I. *Monatsch. Chem.* **1999**, *130*, 731.
- (37) (a) Davis, T. P.; O'Driscoll, K. F.; Piton, M. C.; Winnink, M. A. *Macromolecules* **1989**, *22*, 2785. (b) Beuermann, S.; Bubak, M.; Russel, G. T. *Macromol., Rapid Commun.* **1994**, *15*, 351. (c) Morrison, B. R.; Piton, M. C.; Winnink, M. A.; Gilbert, R. G.; Napper, D. H. *Macromolecules* **1993**, *26*, 4368. (d) Coote, M.; Davis, T. P.; Klumperman, B.; Monteiro, M. *J. Macromol. Sci., Rev. Macromol. Chem. Phys.* **1998**, *C38*, 567. (e) Also in ATRP the k_p is solvent independent. See: Chambard, G.; Klumperman, B.; German, A. L. *Macromolecules* **2002**, *35*, 3420.
- (38) McKenna, T. F.; Villanueva, A.; Santos, A. M. *J. Polym. Sci., Part A: Polym. Chem.* **1999**, *37*, 571.
- (39) (a) Kamachi, M.; Liaw, D.; Nozakura, S. *Polym. J.* **1979**, *11*, 921. (b) Kamachi, M. *Adv. Polym. Sci.* **1981**, *38*, 55. (c) Kamachi, M. *Adv. Polym. Sci.* **1987**, *82*, 209.
- (40) (a) Czerwinski, W. K. *Makromol. Chem. Theory Simul.* **1993**, *2*, 577. (b) Czerwinski, W. K. *Makromol. Chem.* **1991**, *192*, 577. (c) Czerwinski, W. K. *Makromol. Chem.* **1992**, *193*, 359. (d) Czerwinski, W. K. *Makromol. Chem.* **1993**, *194*, 3015. (e) Czerwinski, W. K. *Macromolecules* **1995**, *28*, 5405. (f) Czerwinski, W. K. *Macromolecules* **1995**, *28*, 5411. A serious disadvantage of this model is the large number of optimizable parameters.
- (41) Lucarini, M.; Pedulli, G. F.; Valgimigli, L. *J. Org. Chem.* **1998**, *63*, 4497.
- (42) Snelgrove, D. W.; Luszyk, J.; Banks, J. T.; Mulder, P.; Ingold, K. U. *J. Am. Chem. Soc.* **2001**, *123*, 469.
- (43) (a) Matsumoto, A.; Mohri, Y. *J. Polym. Sci., Part A: Polym. Chem.* **1999**, *37*, 2803. (b) Plochocka, K. *J. Macromol. Sci., Rev. Macromol. Chem.* **1981**, *C20*, 67.

MA021785R